Geomechanics and Engineering, *Vol. 12, No. 6 (2017) 899-917*
DOI: https://doi.org/10.12989/gae.2017.12.6.899

Experimental study on axial response of different pile materials in organic soil

Hanifi Canakci [1a] and Majid Hamed [*1,2]

[1] *Department of Civil Engineering, Gaziantep University, Gaziantep, Turkey*
[2] *Department of Civil Engineering, Kirkuk University, Kirkuk, Iraq*

(*Received March 21, 2016, Revised November 11, 2016, Accepted January 06, 2017*)

Abstract. Sixty four tests were performed in a steel tank to investigate the axial responses of piles driven into organic soil prepared at two different densities using a drop hammer. Four different pile materials were used: wood, steel, smooth concrete, and rough concrete, with different length to diameter ratios. The results of the load tests showed that the shaft load capacity of rough concrete piles continuously increased with pile settlement. In contrast, the others pile types reached the ultimate shaft resistance at a settlement equal to about 10% of the pile diameter. The ratios of base to shaft capacities of the piles were found to vary with the length to diameter ratio, surface roughness, and the density of the organic soil. The ultimate unit shaft resistance of the rough concrete pile was always greater than that of other piles irrespective of soil condition and pile length. However, the ultimate base resistance of all piles was approximately close to each other.

Keywords: organic soil; pile driving; pile roughness; pile load capacity

1. Introduction

Piles are always subjected to axial forces due to its weight as well as additional loads, which are axially transferred to the pile through its shaft and base. Therefore, it is important to examine pile responses under axial loading. The use of pile foundations is perhaps the oldest method of structure construction on soft soils. Piles are stiff members that are generally made of steel, concrete, or timber. Once installed, these geotechnical structures are used to transmit surface loads to a strong soil layer at depth (end-bearing piles) or to spread the loads through the soil (friction piles) when surface soils are soft or too loose to a support shallow foundation safely and economically (Das 2007). When one or more upper soil layers are highly compressible and too weak to support the load transmitted by a superstructure, piles are used to transmit the load to underlying bedrock or a stronger soil layer. When bedrock is not encountered at a reasonable depth below the ground surface, piles are used to transmit the structural load to the soil gradually. Any resistance to the applied structural load is derived mainly from the frictional resistance developed at the soil-pile interface (Vesic 1977). Organic soils have long been documented as problematic soil, because of their high compressibility, low shear strength, considerable secondary

*Corresponding author, Ph.D. Student, E-mail: macid79@gmail.com
[a] Ph.D., E-mail: canakci@gantep.edu.tr

http://www.techno-press.org/?journal=gae&subpage=7 ISSN: 2005-307X (Print), 2092-6219 (Online)

consolidation deformations and permeability. Since it is much weaker and more compressible than inorganic soils, and thus do not provide suitable support for most engineering projects (Coduto 1999, Hwang *et al*. 2005). If such soil is present, we usually avoid them, excavate them, or drive piles through them to reach more suitable deposits (Coduto 1999).

Full-scale field tests are highly desirable, but they are generally expensive, difficult to perform and time consuming. In the absence of resources, laboratory tests are generally conducted with small piles in test bins or tanks. The laboratory tests are popular because they are inexpensive, easy to organize, and independent of the weather. Studies on the behavior of a single pile in laboratory tests under static loading have received extensive attention from previous researchers. Kerisel and Adam (1962) studied the behavior of single pile in situ tests and determined the factors that affect the bearing capacity of a single pile. These factors included density, depth, diameter of the pile and loading rate. The influence of axially loaded piles on the ultimate shaft friction and load-displacement response in clay was also studied by Karlsrud (2014). Lee *et al*. (2011) studied the effect of axial loads on the lateral response of piles driven in sand. The work revealed that the presence of an axial load on a driven pile is detrimental to its lateral capacity, for the lateral deflection of the model pile head increased with increasing axial load. Akgüner and Kirkit (2012) studied the effect of axial loading on the bearing capacity of socketed cast-in-place pile to compare with empirical methods; they reported that the bearing capacities obtained from the empirical correlations agree reasonably well with those calculated from pile load tests. Barari *et al*. (2015) studied the interaction of fluid-structures-seabed of a monopile foundation of wind turbine in liquefiable soils, they used finite difference program to investigate the mechanisms of the monopiles in saturated granular soil. The axial pile capacity is predicted from unit shaft and toe resistances, increasing linearly with depth, but reaching a "limiting value" or "critical depth" after a certain depth (Leland and Kraft 1991). Stringer and Madabhushi (2012) investigated the transfer of axial load during a liquefaction event, they found that shaft friction continues to be maintained during an earthquake in both loose and dense soil. Li *et al*. (2012) have studied the effect of previous cyclic axial loads on the performance of pile groups subjected to subsequent cyclic lateral loads. Many researchers (Horvath 1995, Al-Mhaidib 2001) have investigated the effect of loading rate on axial pile capacity. Paik *et al*. (2011) studied the axial responses of tapered piles in sandy soil, they showed that the shaft load of tapered piles continuously increased with pile settlement.

It was found from the literature review that there is lack of research on the behavior of pile in organic soil. Hence, in this paper, load tests were carried on out on piles to investigate the effect of pile materials and density on axial loads capacity of single piles driven into organic soil. The testing program involves four types of circular piles namely steel, wood, smooth concrete and rough concrete—a square steel soil tank, a driving and loading system. During driving of the pile with a drop hammer, the pile penetration per hammer blow was measured in order to evaluate pile drivability at different densities and pile types.

2. Experimental setup

The tests described in this paper depend on the use of a soil tank, a pile driving system, and piles, each of which will be described subsequently.

2.1 Soil tank and pile driving system

Fig. 1 shows soil tank, piles and loading system used in this study. The soil tank is a square steel tank with a dimension of 800 mm × 800 mm × 800 mm. In order to avoid a boundary effect, a radial boundary larger than a seven-pile diameter and a vertical boundary of a four-pile diameter between pile toe and base of the container were selected. (Vipulanandan *et al*. 1989) Considering these limitations, four piles were tested in the tank. Similar orders of testing were also adopted in the studies reported by Amde *et al*. (1997), El Naggar and Sakr (2002), Banerjee *et al*. (2014). The soil tank has two main parts: a guide leader for pile driving and a loading frame that consists of four vertical columns of 1.0 m height, two on each side and two supports for setting up a reaction beam. The reaction beam consists of hand operated hydraulic jack that can be fixed at each point along it. Calibrated proving of 4.5 kN capacity was attached to the jack to measure the applied load. A jack was used manually to produce the incremental loading. In order to record the correct vertical settlement of the footings for each load increment applied, two sensitive dial gauges of the least measurement, 0.01 mm, were used, and their average was taken. The dial gauges were mounted on rigid rectangular steel tube fixed at the upper edges of the tank.

The pile driving system consists of a pile guide leader, a pile driving head, a hammer rod, and a drop hammer. The main function of the pile guide leader is to maintain proper vertical alignment of the model pile during driving. It is mounted such that it can be moved in the horizontal direction as needed to allow driving of the model pile at any location in the soil sample. The pile driving head protects the pile head from damage during driving, especially when using concrete pile. The guide rod is connected with a driving rod in a manner so that there are no eccentric hammer

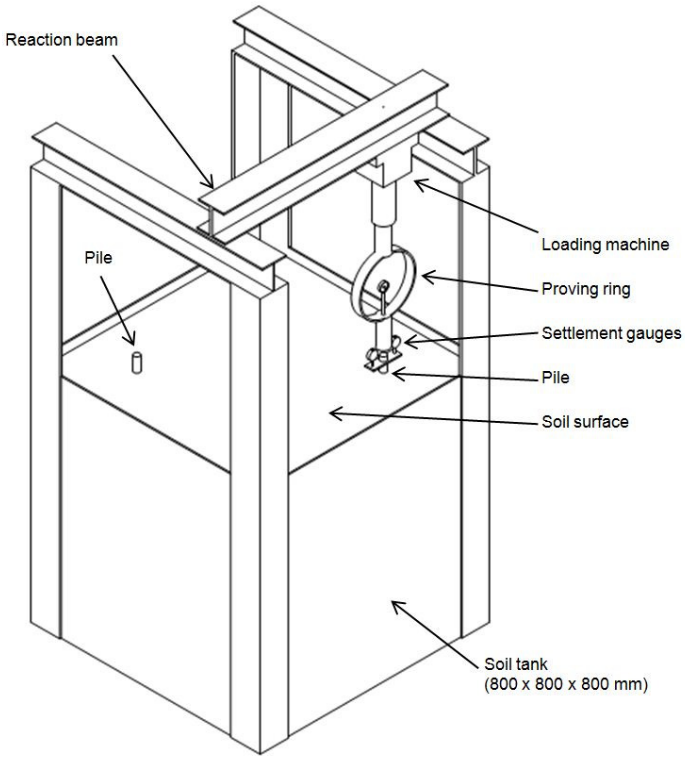

Fig. 1 Loading system includes reaction beam, manual hydraulic jack, calibrated proving ring, and two dial gauges for measuring settlement

blows. During the pile driving, the drop hammer 21.5 N, which consists of two assembled steel cylinder with a concentric circular hole used for loose and dense cases, is inserted into the guide rod and dropped from a fall height of 600 mm. The reaction beam, which is a 120-mm-wide H-beam fabricated from 12-mm-thick steel plates, is detachable from the soil tank and can slide along the whole tank. It is mounted and bolted to the supports on the soil tank. At the end of each experiment, the compacted soil in the tank is removed.

2.2 Piles and pile casing

In order to study the influence of the length and type of pile on the axial response of piles, four types of pile were used in the tests; namely steel pipe, wood, smooth concrete, and rough concrete (Fig. 2). The diameter of the piles was selected as 20 mm according to a suggestion made by Vipulanandan *et al*. (1989). According to the author, pile-to-particle diameter ratio should be at least 50. Loukidis and Salgado (2009) showed that this ratio must be at least in the order of 100 in order to minimize shaft resistance scale effects. In this study, the ratio of the model pile diameter (20 mm) to the average sand particle diameter (D_{50} = 0.017 mm) is 1176. This ratio is greater than the values suggested in the literature. The lengths of piles used for the study are 100, 200, 400, and 600 mm. These lengths represent the L/D ratio (length to diameter ratio) of 5, 10, 20, and 30 respectively, plus the free standing length of 50 mm for avoiding contact of the flat bottom of the piston load that touches the pile head with the soil. This would ensure that the behavior measured from the experiments is only due to the interaction of the pile and soil. A pile casing was used in the tests as a technique to measure the base load capacity of piles, since this technique was used to isolate the pile shaft from the surrounding soil.

Pile casing is a hollow steel tube with a diameter larger than the pile's diameter and both sides are open ended. They also have different lengths, as in the pile model, except that it is smaller than the pile length (no free standing length) in order to prevent the touching that may occur with the load piston during testing. A steel rod with closed ends was inserted inside the casing and was held together during driving using bolts. The purpose of the rod was to compact the soil under the pile base during driving of pile casing; that will give approximately the same bed density obtained during driving of the pile without casing. This rod will be removed after the deriving of pile casing is completed and replaced with the required length and type of pile.

(a) (b) (c) (d)

Fig. 2 Types pile used for tests (a) wood pile; (b) steel pile; (c) smooth surface concrete pile; and (d) rough surface concrete pile

2.3 Fabrication of piles

A steel pipe with an outer diameter of 20 mm and a 2.5 mm wall thickness is cut into the required length for simulating the desired length-to-diameter ratio of the pile. Pipe pile has been used in many studies (Khare and Gandhi 2009, El-Garhy *et al*. 2013). The same manner was used to prepare the wood pile. Two precast reinforced concrete circular piles with different surface conditions (smooth and rough) were designed and fabricated; similar concrete piles were manufactured by Chow and Wong (2004), Faizi *et al*. (2015), Tang and Ling (2014). The reinforced concrete piles were cast using steel pipes with 20 mm internal diameter. It was divided into two halves, which were used as a mold and fresh concrete was poured inside it. The two halves were removed 72 hours after casting to get a proper model pile without any damage during mold removing. The reinforced-concrete piles were fabricated with fine-aggregate concrete, steel bar and galvanized fine iron wires. A single steel bar with a diameter of 5 mm was used as longitudinal reinforcement and placed at the center of pile cross section, as shown in Fig. 2. Plain iron wires with a diameter of 1.5 mm and spaced at a pitch of 20 mm were used as spiral reinforcements in a diameter of 12 mm for each pile. The piles were cured for 28 days before they were tested. The average unconfined compressive strength of the three concrete cube samples tested (50 × 50 × 50 mm) was 53 MPa.

Surface roughness of the pile materials was then calculated. The method adopted to measure the surface roughness was estimated by using dial gage in this study. This dial gage was moved along the pile surface in a straight line and then the readings were taken and recorded. The average roughness (Ra) value defined as the arithmetic mean of the departures of the profiles from the main line (Fig. 3). The rough surface for concrete was created by bonding sand grains to their shafts, sand grains were glued to the pile shafts to create 'fully rough' interfaces (Lehane and Schneider 2005, Lim and Lehane 2014). The measured values are given in Table 1.

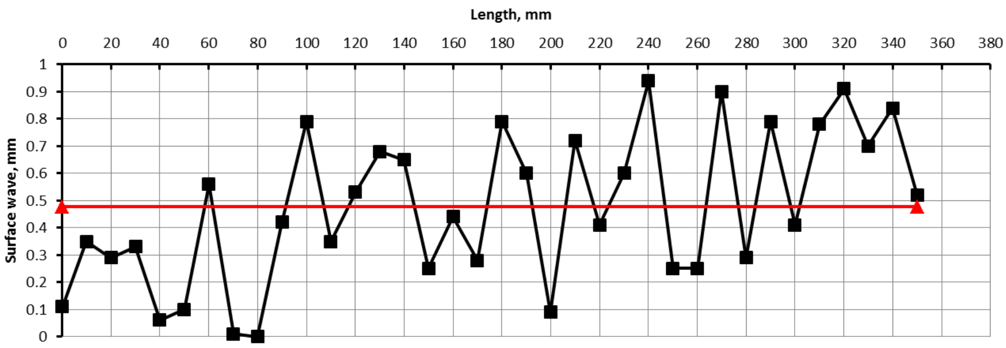

Fig. 3 Surface waves with respect to surface length for rough concrete pile

Table 1 Properties of material used

Material No.	Type of material	Average roughness, Ra (μm)
1	Steel	36.4
2	Wood	47.3
3	Smooth concrete	60.4
4	Rough concrete	199.2

Table 2 Classification of organic soil based on ASTM

ASTM Standard	Criteria	Designation	Present Study
Fiber Content (D1997)	> 67% fibers Fibric (H1-H3)	> 67% fibers	22.31% Sapric (H7-H10)
	Hemic (H4-H10)	33%-67% fibers	
	Sapric (H7-H10)	< 33% fibers	
Ash Content (D2974)	Low ash	< 5% ash	77% high ash
	Medium ash	5%-15% ash	
	High ash	15% < ash	
Acidity (D2976)	Highly acidic	pH < 4.5	6.7 slightly acidic
	Moderately acidic	4.5 < pH < 5.5	
	Slightly acidic	5.5 < pH < 7	
	Basic	pH > 7	

Table 3 Properties of the organic soil presented in this study

Item	Quantity
Organic Content	23%
PH	6.7
Effective size (D_{10})	0.007
Mean particle size (D_{50})	0.017
Maximum dry density*	10.3 kN/m^3
Optimum water content*	39%
Liquid limit	75%
Plastic limit	45%
Natural water content	97%
Fine sand	23.4%
Clay and silt	76.6%
Specific gravity	2.24

*Maximum dry density and optimum water content were obtained according to standard compaction test ASTM D698-12 (2014)

3. Material and method

3.1 Properties of the organic soil

The organic soil used in this study was obtained from the Sakarya region of Turkey. The organic content (OC) of the soils was measured by ignition in a muffle furnace at 440° C for 4 hours, according to ASTM D2974. The natural organic soils are classified according to ASTM and with other different classification systems (Table 2). Table 3 presents the physical properties of the soil.

3.2 Soil bed preparation and pile driving

Density of the organic soil in the test tank was achieved by compaction. For this purpose, the height of the tank was divided into layers of 50 mm. The specific weight of soil was placed in the tank for each layer to obtain two different relative densities, 75% and 50%, respectively. At these densities, unit weights of compacted organic soil in the tank were 7.73 kN/m^3 and 5.2 kN/m^3, respectively. The water content was kept 30% for all the tests. This method was adopted from previous experiments (Amde *et al*. 1997, Rao and Nasr 2010, El-Garhy *et al*. 2013). The top 35 mm of the tank remained empty to avoid soil overflow. The final height of the prepared soil samples was about 770 mm. After sample preparation, the pile was driven in the soil sample to a penetration depth according to the required length of the tested pile, using the guide rod and steel hammer described previously. The driving energy considered for dense and loose case was 21.5 Nm (2.23-kg-hammer weight), and 600 m drop height for all cases. In order to evaluate pile drivability in soil samples prepared at different densities, the blow count required for driving the pile into the soil sample and the penetration per hammer blow (i.e., the pile set) was recorded during pile driving. After driving the pile, the driving system was removed from the reaction beam and the jack with a proving ring was assembled onto the reaction beam to build a system of axial reaction for the load tests. The load tests were carried out immediately following driving to prevent time-dependent pile set-up effects. The axial loads applied to the pile head were measured by the calibrated proving ring. The vertical pile head displacement was monitored using two dial gages. The vertical load was increased with constant load increments of 0.03 kN. After each loading increment, the applied load was maintained constant until the vertical displacement stabilized. To measure the pile base only (Fig. 4), the procedure used for pile driving was used for pile casing. Grease was used to lubricate the pile skin, to avoid any friction that may have occurred between pile skin and inside wall of the casing. This technique used to measure pile base in the loose and dense cases to know the degree of contribution of the base and shaft to the total load capacity.

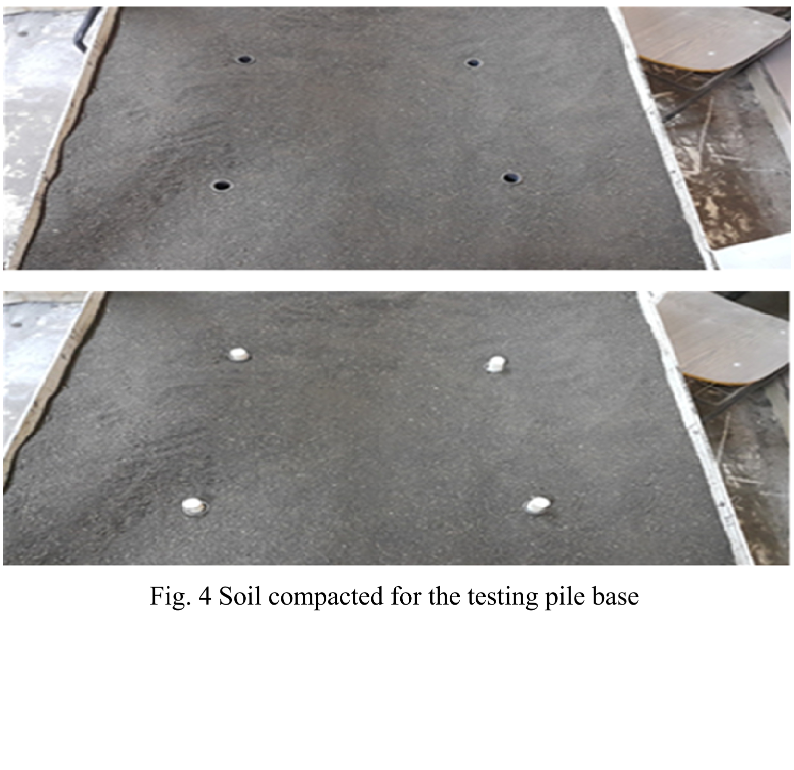

Fig. 4 Soil compacted for the testing pile base

Table 4 Summary of test parameters and their values

Constant parameters	
Test device	Soil tank (800 mm × 800 mm × 800 mm)
Soil type	Organic soil
Pile	Pile diameter 20 mm
Variable parameters	
Pile type	Wood, steel, smooth concrete, and rough concrete
Pile length (L/D)	10 mm (5), 20 mm (10), 40 mm (20), and 60 mm (30)
Soil density	Loose, dense

Table 5 Program of pile tests

Soil case	Type of test	Pile type	L/D ratio	Test number
Loose case	Total capacity measurement	Wood	5, 10, 20, 30	4
		Steel	5, 10, 20, 30	4
		Smooth concrete	5, 10, 20, 30	4
		Rough concrete	5, 10, 20, 30	4
Dense case	Total capacity measurement	Wood	5, 10, 20, 30	4
		Steel	5, 10, 20, 30	4
		Smooth concrete	5, 10, 20, 30	4
		Rough concrete	5, 10, 20, 30	4
Loose case	Base capacity measurement	Wood	5, 10, 20, 30	4
		Steel	5, 10, 20, 30	4
		Smooth concrete	5, 10, 20, 30	4
		Rough concrete	5, 10, 20, 30	4
Dense case	Base capacity measurement	Wood	5, 10, 20, 30	4
		Steel	5, 10, 20, 30	4
		Smooth concrete	5, 10, 20, 30	4
		Rough concrete	5, 10, 20, 30	4
			Total	64

4. Test program

The testing program included a parametric study that investigated different variables. Table 4 shows a summary of these test parameters and their values. The total number of tests performed was 64, as shown in Table 5. In addition to these tests, a few tests were repeated to check the reputability of the test results; similar results were found.

5. Test results

5.1 Pile drivability

The drivability of the piles was investigated in dense and loose soil cases. Figs. 5 and 6 show the cumulative blow count versus pile penetration depth and the penetration per blow of the pile, respectively, for each soil sample. The cumulative hammer blows count for rough concrete exceeded smooth concrete, steel, and wood in both dense and loose cases. The average set (penetration per blow) was 0.88, 0.56, 0.6, and 0.44 cm for wood, steel, smooth concrete, and rough concrete, respectively, in the dense case. In the loose case, these values were 2.74, 2.03, 0.94, and 0.72, respectively. As can be seen in Fig. 5, the rate of penetration decreased as the pile penetrated deeper into the soil because of higher pile surface area contact with soil. Lee *et al.* (2011), Giraldo and Rayhani (2014) also reported the same results in their studies. Fig. 5 also shows that as the penetration depth increased, especially after L/D ratio greater than 15, the rate of penetration in rough concrete, smooth concrete, and steel approached each other, while that approach was not achieved in wood until it reached an L/D ratio equal to 25 in the dense case. The rates of penetration for the rough and smooth concrete piles were close to each other when the penetration reached L/D ratio of 10 in the loose case. This behavior was also observed in steel and wood pile.

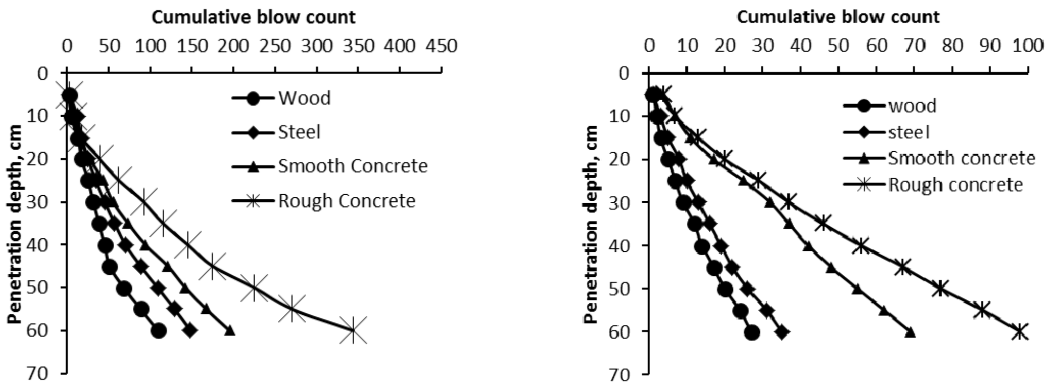

(a) Dense soil (b) Loose soil

Fig. 5 Cumulative blow count versus the penetration depth of the pile driven into organic soil

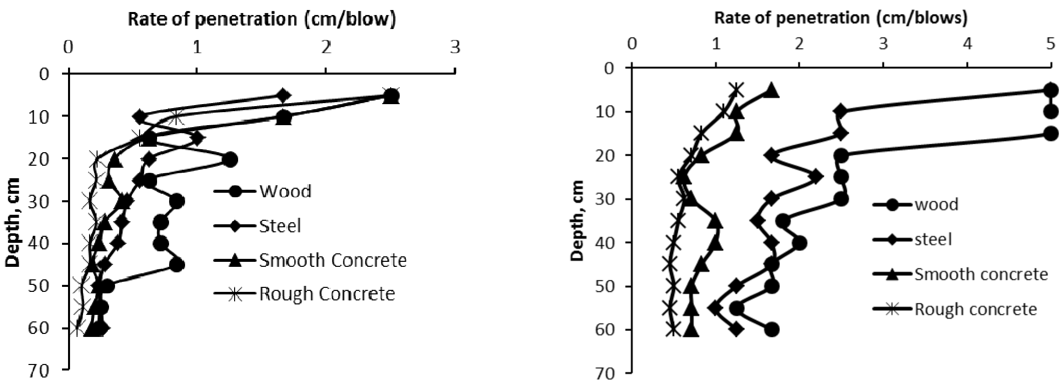

(a) Dense soil (b) Loose soil

Fig. 6 Rate of pile penetration versus the penetration depth

5.2 Load - Displacement behavior

Pile load test results are summarized in Figs. 7 and 8, in which axial load capacity is plotted against vertical pile head displacement. Ultimate pile capacity was defined as the load corresponding to a pile head displacement equal to 10% of the pile diameter (De Nicola and Randolph 1999). The loading behavior of all piles was similar, and has a general trend. The axial load tests were terminated when the pile plunged into the soil. In all cases, ultimate capacity for all the pile types in the dense case ranged from 2.5 to 3.5 times that of loose soil. Rough concrete pile presented the fastest rate of capacity increase, while the steel and wood piles presented the most gradual increases. The rapid change in slope of the load-displacement curve after the early portion of loading can be attributed to the frictional failure of the soil surrounding the pile shaft (Giraldo and Rayhani 2014). The results of present study were compared with previous works (Kouby *et al.* 2013, Patil *et al.* 2015) done on sand (Table 6), as shown in Fig. 9. It is seen in Fig. 9 that there is a significant difference in the ultimate load capacity of the tested piles. For all types of piles used in this study at the same L/D ratio, ultimate load capacity is lower in organic soil. This may be because the type of soil in this work is weaker than that of sand, in which most of the pile tests

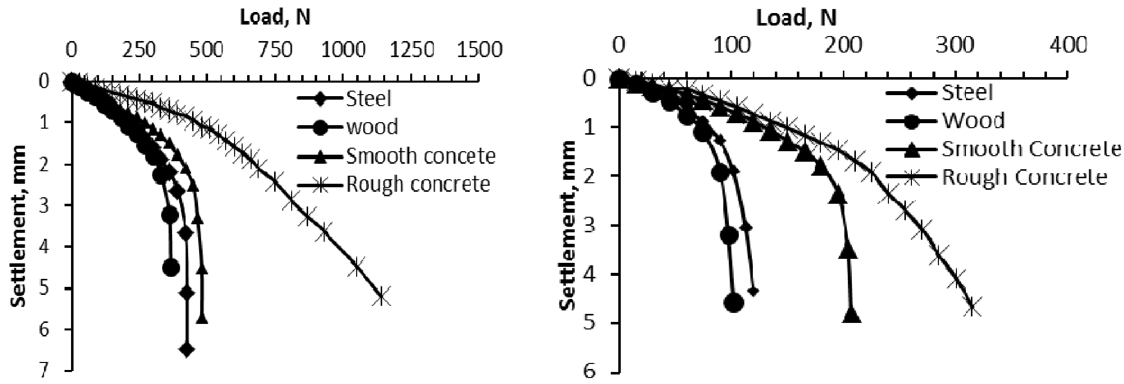

(a) Dense soil (b) Loose soil

Fig. 7 Load-settlement curve for L/D = 30

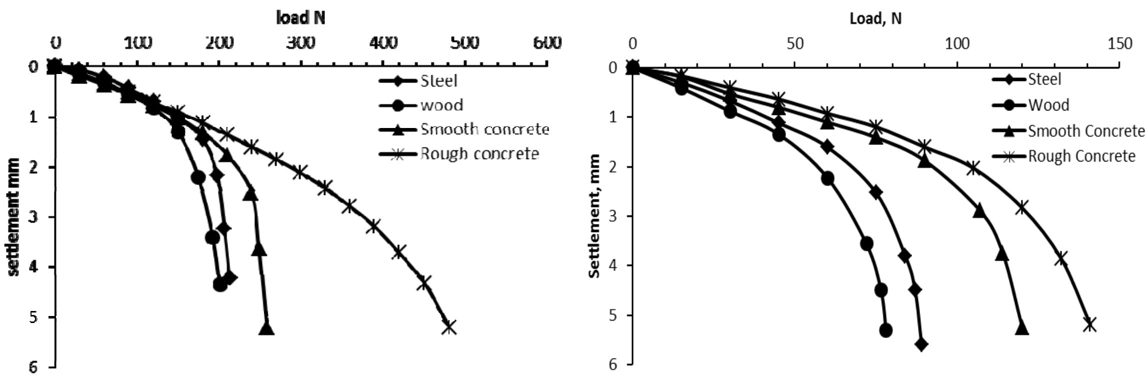

(a) Dense soil (b) Loose soil

Fig. 8 Load – settlement curve for L/D = 10

Table 6 A summary of some axial load tests on instrumented model piles described in the load-settlement

Reference	Pile configuration	Soil type	Pile geometry		Dimensions of soil tank
			Diameter mm	Length mm	mm
Kouby *et al*. (2013)	Single pile	Sand	20	735	Diameter = 524 Height = 700
Patil *et al*. (2015)	Single pile	Sand	20	200	Length = 850 Width = 850 Height = 500

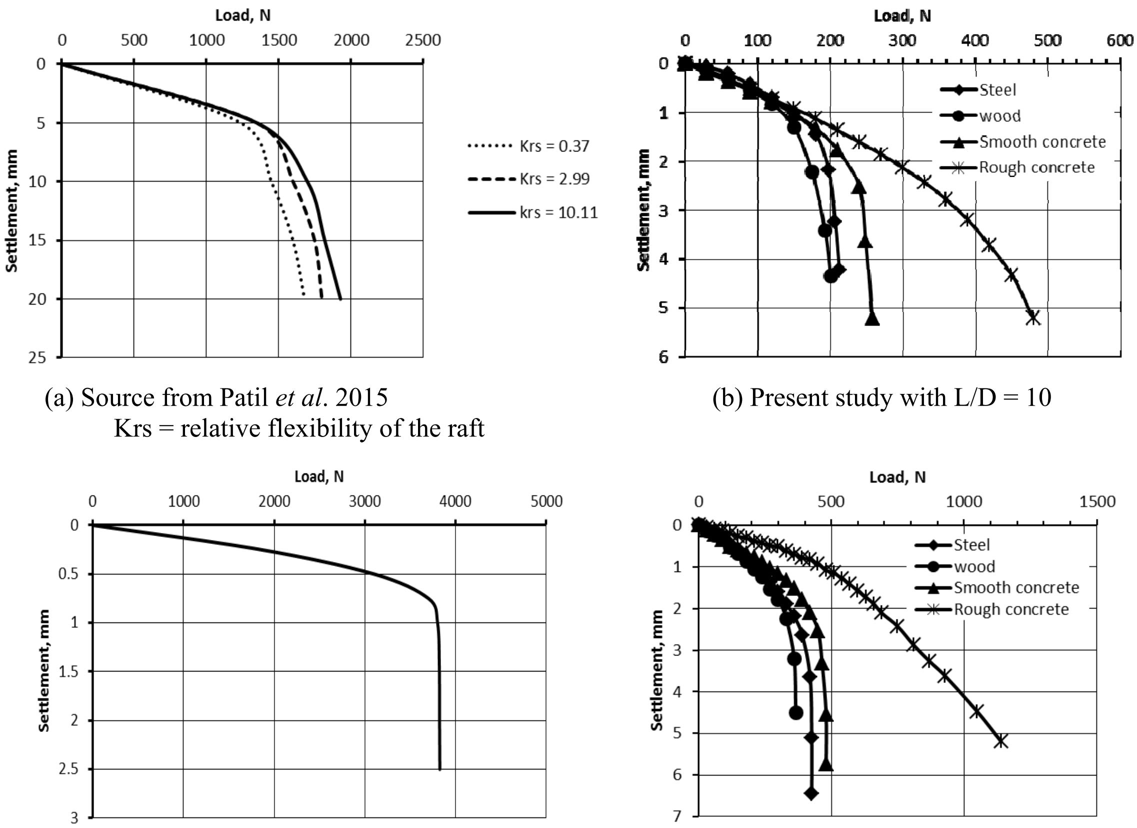

(a) Source from Patil *et al*. 2015
Krs = relative flexibility of the raft

(b) Present study with L/D = 10

(c) Source from Kouby *et al*. 2013

(d) Present study with L/D = 30

Fig. 9 Comparison of load-settlement behavior of present study with different source papers

were performed. Other reasons may be pile stiffness, material, and degree of compaction of the proposed soil.

5.3 Base and shaft load capacities

Figs. 10-13 show the base, shaft, and total load versus pile head displacement curves for the piles driven into loose and dense soil. The ultimate base and shaft resistance values of the test piles

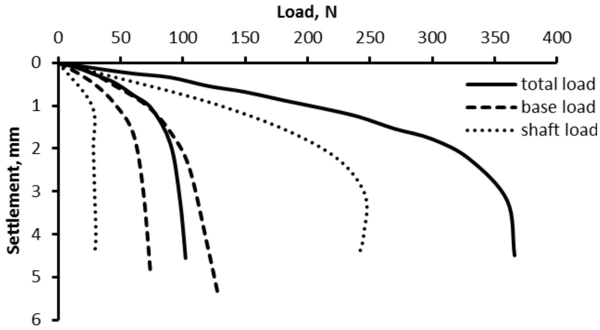

Fig. 10 Total, base and shaft load versus pile head settlement for wood pile (L/D = 30)

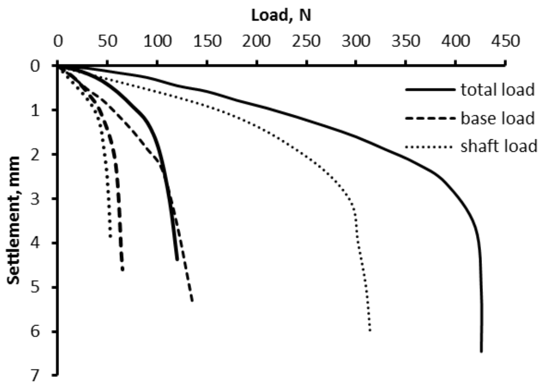

Fig. 11 Total, base and shaft load versus pile head settlement for smooth concrete pile (L/D = 30)

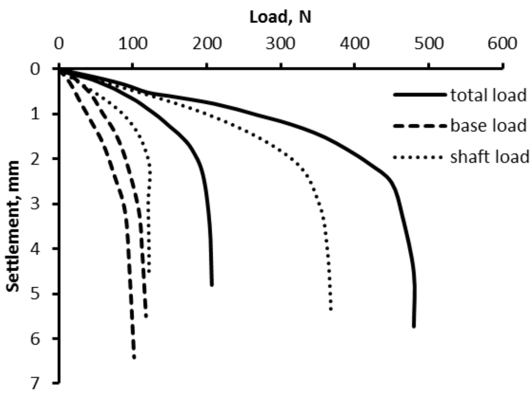

Fig. 12 Total, base and shaft load versus pile head settlement for steel pile (L/D = 30)

are defined as the base and shaft loads per unit area of the pile at a settlement of about 2 mm; the outcome corresponds to 10% of the pile diameter. The base load capacity was measured directly using the proving ring at the pile head, whereas the shaft capacity was computed by subtracting the base load from the total load applied to the pile head. As can be seen in Figs. 10-13, the shaft resistance was fully mobilized when the pile head displacement was about 5-10% of pile diameter.

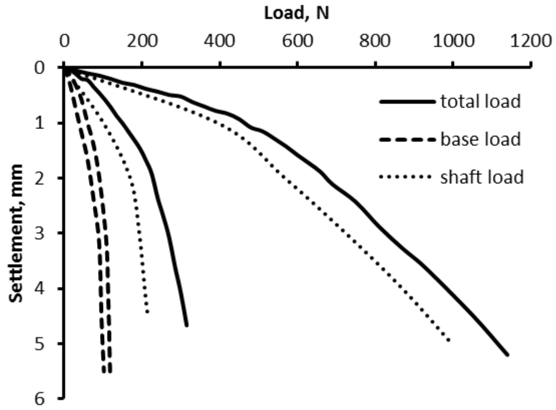

Fig. 13 Total, base and shaft load versus pile head settlement for rough concrete pile (L/D = 30)

Table 7 Total, base and shaft load in loose soil

Pile type	L/D	Total load N	Base load N	Shaft load N	Load ratio	
					Qb/Qt	Qs/Qt
Wood	5	32	30	2	0.938	0.063
	10	57	52	5	0.912	0.088
	20	77	60	17	0.779	0.221
	30	90	66	24	0.733	0.267
Steel	5	37	28	9	0.757	0.243
	10	68	49	19	0.721	0.279
	20	86	52	34	0.605	0.395
	30	102	55	47	0.539	0.461
Smooth concrete	5	60	36	24	0.600	0.400
	10	90	54	36	0.600	0.400
	20	130	58	72	0.446	0.554
	30	190	65	125	0.342	0.658
Rough concrete	5	80	39	41	0.488	0.513
	10	106	50	56	0.472	0.528
	20	180	56	124	0.311	0.689
	30	230	68	162	0.296	0.704

The difference of shaft resistance comes from pile length. The higher value was obtained with a high L/D ratio. For the rough concrete pile, shaft load capacity increased continuously with pile settlement of about 25% of the pile diameter. The ultimate shaft load also increased as pile length increased. Tables 7-8 summarize the pile capacity for all pile types. These tables show how the ultimate base and shaft resistance of the test piles increased with the pile length and soil density. Figs. 14-16 show the ratios of the ultimate base load (Qb) and ultimate shaft load (Qs) to the total load capacity (Qt) for piles as a function of soil density and the L/D ratio of piles. It is apparent

Table 8 Total, base and shaft load in dense soil

Pile type	L/D	Total load N	Base load N	Shaft load N	Load ratio	
					Qb/Qt	Qs/Qt
Wood	5	122	43	79	0.352	0.648
	10	170	58	112	0.341	0.659
	20	255	85	170	0.333	0.667
	30	315	93	222	0.295	0.705
Steel	5	138	40	98	0.290	0.710
	10	195	55	140	0.282	0.718
	20	270	71	199	0.263	0.737
	30	340	84	256	0.247	0.753
Smooth concrete	5	160	44	116	0.275	0.725
	10	222	60	162	0.270	0.730
	20	312	78	234	0.250	0.750
	30	410	90	320	0.220	0.780
Rough concrete	5	195	40	155	0.205	0.795
	10	290	60	230	0.207	0.793
	20	425	80	345	0.188	0.812
	30	660	92	568	0.139	0.861

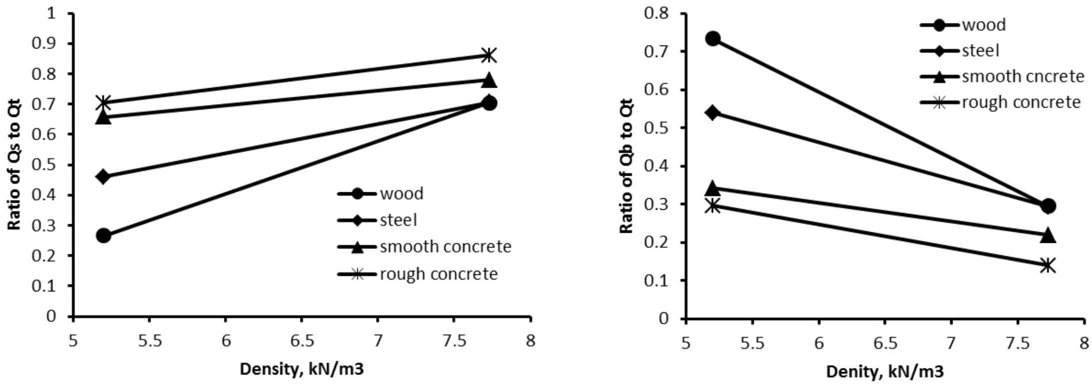

Fig. 14 Ratios of base and shaft to total load capacity versus soil density for L/D = 30

from these figures that the ratio of base to total load capacity for all piles decreases with increasing soil density. Additionally, it was found that the values of Qb /Qt and Qs /Qt can vary depending on pile length. For example, if the pile diameter and soil condition are the same, Qs/Qt will be higher for long piles than short piles. A similar trend was reported by Paik *et al*. (2011). The rough concrete pile has a greater shaft load capacity than other piles for a given soil density and L/D ratio, and always has a low base load capacity compared with its shaft capacity. Therefore, the contribution of the shaft to the total load capacity for rough concrete piles is greater than that for other piles. These experimental results are consistent with the results of Giraldo and Rayhani

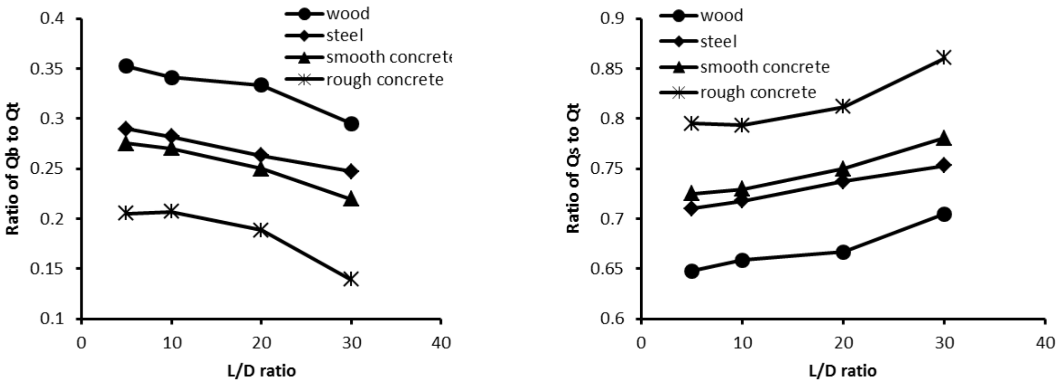

Fig. 15 Ratios of base and shaft to total load capacity versus L/D ratio for loose soil

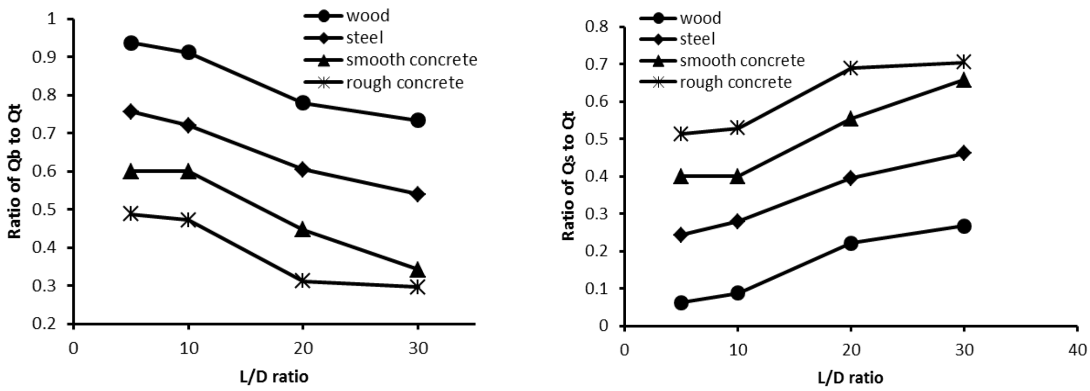

Fig. 16 Ratios of base and shaft to total load capacity versus L/D ratio for dense soil

(2014). The higher shaft resistances of rough concrete piles are attributed to their surface roughness compared to the smooth concrete, wood and steel piles. Pile surface texture plays a significant role in the increased shaft resistance, because textures in the pile fabric create increased contact area between the soil and pile. It can be concluded that rough concrete piles would be more effective in the aspect of load capacity when they are used as friction piles, compared to when they are used as end bearing piles. From these figures, it can be observed that the values of Qb /Qt and Qs /Qt vary depending on pile length and soil density.

5.4 Effect of pile length

The pile length has a major influence on the bearing capacity of single piles. It can be clearly observed from Fig. 17 that for a particular relative density, the bearing capacity increases significantly with an increase of L/D ratio. Tests were conducted for different pile materials with two different densities: 7.73 and 5.2 kN/m^3. A summary of the test results is given in Tables 7-8. The variations of ultimate total load with L/D for the two densities are shown in Figs. 17(a)-(b). The results clearly indicate that for both densities, the ultimate load capacities increase with increasing the L/D ratios, along with increasing soil density. This can be attributed to the embedded length for small L/D ratios not being sufficient to create a full mobilize friction of the

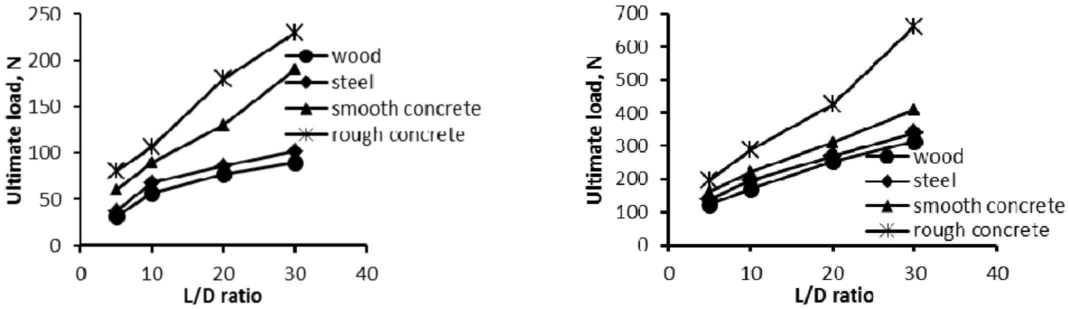

(a) Loose soil (b) Dense soil

Fig. 17 Ultimate load versus L/D ratio

piles to resist the vertical movement from the axial load. Thus, for a grater L/D value, the piles will get enough friction to resist axial load. It is evident that increasing the part of pile length embedded in the underlying soil leads to more stability for the piles and greater resistance for the vertical loading due to axial load. Also, increasing the pile length is more sufficient to increase interface friction between pile surface and surrounding soil. A similar observation has been reported in the results of previous experimental study done by Rao and Nasr (2010).

5.5 Effect of pile type and soil density

Load capacity of the pile depends on the surface characteristics of the soil-pile interface. As shown in Fig. 18, it is well known that the bearing capacity of precast concrete piles (smooth and rough piles) is higher than that of smooth surface (steel and wood piles) in a similar soil density, so that the ultimate bearing capacity depends mainly on the pile material and surface roughness. Based on Fig. 18, it is evident that the soil-pile interface is governed by surface roughness and pile materials (Jardine *et al*. 1998, Paik *et al*. 2011, Giraldo and Rayhani 2014). It is clear that rough concrete pile reached the highest resistance compared to steel and wood piles. This behavior was noticed in the smooth concrete pile but less so in the rough concrete pile. The higher shaft resistances of rough and smooth concrete piles are attributed to their surface roughness compared to those of the steel and wood piles. Pile surface texture plays a significant role in the increased

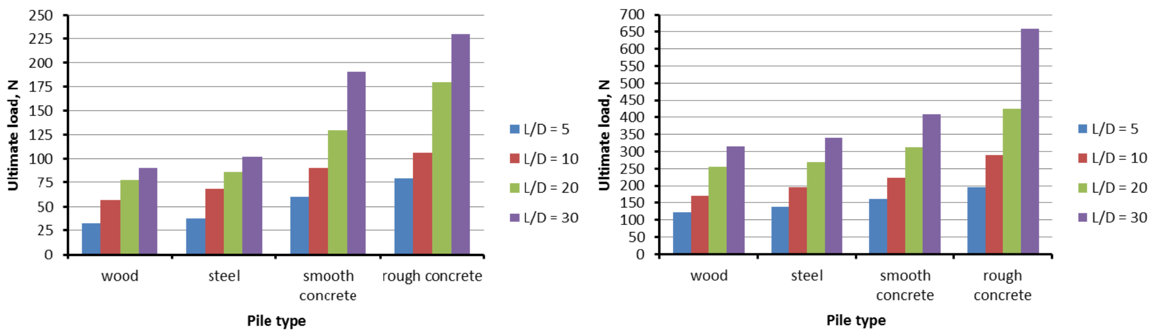

(a) Loose soil (b) Dense soil

Fig. 18 Ultimate load versus pile type of different pile materials

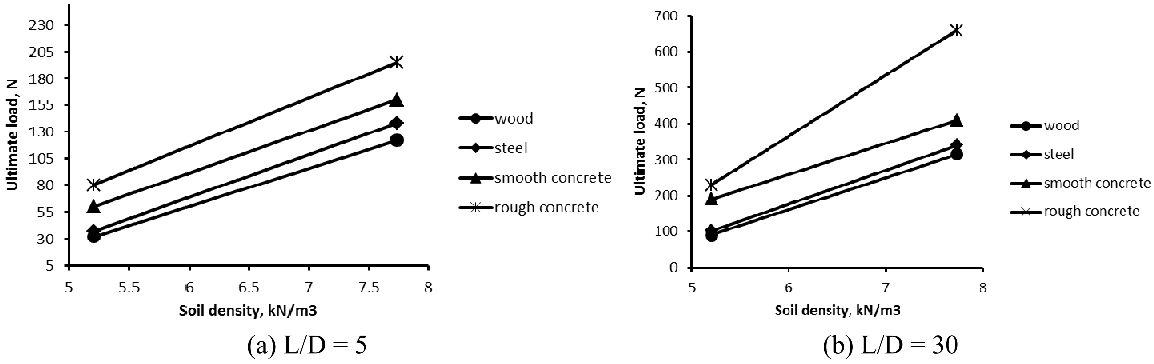

Fig. 19 Ultimate bearing capacity versus soil density

shaft resistance, because textures in the pile fabric create an increased contact area between the soil and pile. As seen in Fig. 18 the ultimate load of both steel and wood piles are quite comparable. Although the wood pile has a roughness coefficient higher than that of the steel pile, the later shows slightly larger bearing capacity. This may be due to the plugging behavior of the steel pile (shaft resistance between the soil and internal wall of steel pile) driven in organic soils. The shear forces between the plug and inside pile can be much higher than the shear strength of the soil due to arching of the soil confined inside the pipe (Paikowsky and Whitman 1990). Tests on piles suggest that the pile skin friction also increases with the density of soil (Coyle and Sulaiman 1967, Alawneh *et al.* 2003). In sum, in the present study, the influence of the shear strength of organic soil on the shear resistance of piles was studied by using two densities of 5.2 and 7.73 kN/m^3. The effect is shown in Fig. 19, and is greater for the concrete pile (rough and smooth) than for the wood and steel pile.

6. Conclusions

In this study, 64 pile load tests were carried out in a steel tank to investigate the axial behavior of different pile types in organic soil having two different densities. The main purpose of these tests was to investigate the characteristics of the axial load capacity of piles through comparison of pile material and surface roughness. The conclusions drawn from this study can be summarized as follows:

- The shaft load of smooth surface piles (wood, steel and smooth concrete) reaches the ultimate value at a settlement of around 5% and 10% of the pile diameter for loose and dense states, respectively. Whereas, the shaft load of rough concrete piles increases continuously with pile settlement even at a settlement corresponding to about 15-20% of the average pile diameter for loose and dense soil.
- The ratios of base and shaft to total load capacity of piles significantly depend on the density of soil, pile embedment length and roughness of pile surface. On the other hand, the shaft load capacity ratio increases with increasing soil density and embedment pile length and approaches a value of 1.0 for rough concrete pile, and opposite for base to total capacity ratio.
- The total capacity increase with increasing pile surface roughness, the total capacity for

rough concrete pile was about 2.3, 2 and 1.3 times wood, steel and smooth concrete pile, respectively, for loose soil. This ratio was decreased with the increasing soil density and became a ratio of about 1.6.

References

Akgüner, C. and Kirkit, M. (2012), "Axial bearing capacity of socketed single cast-in-place piles", *Soils Found.*, **52**(1), 59-68.

Alawneh, A.S., Nusier, O.K. and Al-kateeb, M. (2003), "Dependency of unit shaft resistance on in-situ stress: observations derived from collected field data", *J. Geotech. Geol. Eng.*, **21**(1), 29-46.

Al-Mhaidib, A.I. (2001), "Loading rate effect on piles in clay from laboratory model tests", *J. King Saud Univ. (Eng. Sci.)*, **13**(1), 39-55.

Amde, A.M., Chini, S.A. and Mafi, M. (1997), "Model study of H-piles combined loading", *Geotech. Geol. Eng.*, **15**(4), 343-355.

ASTM D2974-13 (2014), Standard Test Methods for Moisture, Ash, and Organic Matter of Peat and Other Organic Soils; West Conshohocken, PA, USA.

ASTM D698-12 (2014), Standard Test Methods for Laboratory Compaction Characteristics of Soil Using Standard Effort; West Conshohocken, PA, USA.

ASTM D1997-91 (2014), Standard Test Methods for Moisture, Ash, and Organic Matter of Peat and Other Organic Soils; West Conshohocken, PA, USA.

ASTM D2976-71 (2013), Standard Test Method for pH of Peat Materials; West Conshohocken, PA, USA.

Banerjee, S., Goh, S.H. and Lee, F.H. (2014), "Earthquake induced bending moment in fixed-head piles in soft clay", *Géotechnique*, **64**(6), 431-446.

Barari, A., Bayat, M., Meysam, S., Ibsen, L.B. and Andersen, L.V. (2015), "Transient analysis of monopile foundations partially embedded in liquefied soil", *Geomech. Eng., Int. J.,* **8**(2), 257-282.

Chow, S.H. and Wong, K.S. (2004), "Model pile pull-out tests using polyethylene sheets to reduce downdrag on cast in situ piles", *Geotech. Test. J.,* **27**(3), 230-238.

Coduto, D.P. (1999), *Geotechnical Engineering: Principles and Practices*, (1st Edition), Prentice Hall, Upper Saddle River, NJ, USA.

Coyle, H.M. and Sulaima, I.H. (1967), "Skin friction for steel piles in sand", *J. Soil Mech. Found. Div., ASCE*, **93**(6), 261-278.

Das, B.M. (2007), *Principles of Foundation Engineering*, (6th Edition), Thomson Canada Limited, Canada.

De Nicola, A. and Randolph, M.F. (1999), "Centrifuge modelling of pipe piles in sand under axial loads", *Géotechnique*, **49**(3), 295-318.

El Naggar, M.H. and Sakr, M. (2002), "Cyclic response of axially loaded tapered pile", *Int. J. Phys. Model. Geotech.*, **2**(4), 1-12.

El-Garhy, B., Galil, A.A., Youssef, A. and Abo Raia, M. (2013), "Behavior of raft on settlement reducing piles: Experimental model study", *J. Rock Mech. Geotech. Eng.,* **5**(5), 389-399.

Faizi, K., Armaghani, D.J., Sohaei, H., Safuan, A., Rashid, A. and Nazir, R. (2015), "Deformation model of sand around short piles under pullout test", *Measurement*, **63**, 110-119.

Giraldo, J. and Rayhani, M.T. (2014), "Load transfer of hollow fiber-reinforced polymer (FRP) piles in soft clay", *Transp. Geotech.*, **1**(2), 63-73.

Horvath, R.G. (1995), "Influence of loading rate on the capacity of a model pile in clay", *Can. Geotech. J.*, **32**(3), 364-368.

Hwang, J., Humphrey, A., Bobet, A. and Santagata, M.C. (2005), Stabilization and Improvement of Organic Soil; Final Report FHWA / IN / JTRP-2004 / 38.

Jardine, R.J., Overy, R.F. and Chow, F.C. (1998), "Axial capacity of offshore piles in dense north sea sands", *J. Geotech. Geoenviron. Eng.,* **124**(2), 171-178.

Karlsrud, K. (2014), "Ultimate shaft friction and load-displacement response of axially loaded piles in clay based on instrumented pile tests", *J. Geotech. Geoenviron. Eng. ASCE*, **140**(12), 1-16.

Kerisel, J. and Adam, M. (1962), "Fondations profondes", Institut Technique du Baˆtiment et des Travaux Publics, Paris,France, Annales de l'Institut Technique du Baˆtiment et desTravaux Publics, se´rie SF, No. 39.
Khare, M.G. and Gandhi, S.R. (2009), "Shear resistance of bitumen-coated piles in sand", *Proceedings of the ICE – Geotech. Eng. J.,* **162**(6), 303-310.
Kouby, A.L., Dupla, J.C., Canou, J. and Francis, R. (2013), "Pile response in sand: experiemental development and study", *Int. J. Phys. Model. Geotech.*, **13**(4), 122-137.
Lee, J., Prezzi, M. and Salgado, M. (2011), "Experimental investigation of the load response of model piles in sand", *Geotech. Test. J.*, **34**(6), 1-15.
Lehane, B.M. and Schneider, J.A. (2005), "Scale effects on tension capacity for rough piles buried in dense sand", *Géotechnique,* **55**(10), 709-719.
Leland, M. and Kraft, J. (1991), "Performance of axially loaded pipe piles in sand", *J. Geotech. Eng.,* **117**(2), 272-296.
Li, Z., Haigh, S.K. and Bolton, M.D. (2012), "Effect of previous cyclic axial loads on pile groups", *Int. J. Phys. Model. Geotech.*, **12**(1), 15-23.
Lim, J.K. and Lehane, B.M. (2014), "Set-up of pile shaft friction in laboratory chamber tests", *Int. J. Phys. Model. Geotech.*, **14**(2), 21-30.
Loukidis, D. and Salgado, R. (2009), "Modeling sand Response using two-surface plasticity", *Comput. Geotech.*, **36**(1), 166-186.
Paik, K., Lee, J. and Kim, D. (2011), "Axial response and bearing capacity of tapered piles in sandy soil", *Geotech. Test. J.*, **34**(2), 1-9.
Paikowsky, S. and Whitman, R. (1990), "The effects of plugging on pile performance and design", *Can. Geotech. J.*, **27**(4), 429-440.
Patil, J.D., Vasanvala, S.A. and Solanki, C.H. (2015), "An experimental study on behaviour of piled raft foundation", *Ind. Geotech. J.*, **46**(1), 16-24.
Rao, S.V. and Nasr, A.M.A. (2010), "Experimental and theoretical studies of vertical piles reinforced sand slopes loaded with strip footing", *Geotech. Test. J.*, **33**(5), 1-12.
Stringer, M.E. and Madabhushui, S.P.G. (2012), "Axial load transfer in liquefiable soils for free-standing piles", *Geotechnique*, **63**(5), 1-10.
Tang, L. and Ling, X. (2014), "Response of a RC pile group in liquefiable soil: a shake-table investigation", *Soil Dyn. Earthq. Eng.*, **67**, 301-315.
Vesic, A.S. (1977), Design of pile foundations; National Cooperative Highway Research Program Synthesis of Practice, No. 42, Transportation Research Board, Washington, DC, USA.
Vipulanandan, C., Wong, D., Ochoa, M. and O'Neill, M.W. (1989), "Modeling of displacement piles in sand using a pressure chamber", *Proceedings of Foundation Engineering Congress*, Reston, VA, USA, pp. 526-541.

CC